

## A Charged Coordination Cage-Based Porous Salt

Eric J. Gosselin, Gerald E. Decker, Alexandra M. Antonio,  
Gregory R. Lorzing, Glenn P. A. Yap, and Eric D. Bloch

*J. Am. Chem. Soc.*, **Just Accepted Manuscript** • Publication Date (Web): 05 May 2020

Downloaded from [pubs.acs.org](https://pubs.acs.org) on May 5, 2020

### Just Accepted

“Just Accepted” manuscripts have been peer-reviewed and accepted for publication. They are posted online prior to technical editing, formatting for publication and author proofing. The American Chemical Society provides “Just Accepted” as a service to the research community to expedite the dissemination of scientific material as soon as possible after acceptance. “Just Accepted” manuscripts appear in full in PDF format accompanied by an HTML abstract. “Just Accepted” manuscripts have been fully peer reviewed, but should not be considered the official version of record. They are citable by the Digital Object Identifier (DOI®). “Just Accepted” is an optional service offered to authors. Therefore, the “Just Accepted” Web site may not include all articles that will be published in the journal. After a manuscript is technically edited and formatted, it will be removed from the “Just Accepted” Web site and published as an ASAP article. Note that technical editing may introduce minor changes to the manuscript text and/or graphics which could affect content, and all legal disclaimers and ethical guidelines that apply to the journal pertain. ACS cannot be held responsible for errors or consequences arising from the use of information contained in these “Just Accepted” manuscripts.

# A Charged Coordination Cage-Based Porous Salt

Eric J. Gosselin, Gerald E. Decker, Alexandra M. Antonio, Gregory R. Lorz, Glenn P. A. Yap, and Eric D. Bloch\*

Department of Chemistry and Biochemistry, University of Delaware, Newark, Delaware 19716, United States

Supporting Information Placeholder

**ABSTRACT:** Metal-organic frameworks and porous coordination cages have shown incredible promise as a result of their high tunability. However, syntheses pursuing precisely targeted mixed functionalities, such as multiple ligand types or mixed-metal compositions are often serendipitous, require post-synthetic modification strategies, or are based on complex ligand design. Herein, we present a new method for the controlled synthesis of mixed functionality metal-organic materials via the preparation of porous salts. More specifically, the combination of potentially-porous ionic molecules of opposite charge affords framework-like materials where the ratio between cationic cage and anionic cage is potentially tunable. The resulting doubly-porous salt displays the spectroscopic signatures of the parent cages with increased gas uptake capacities as compared to starting materials. This approach will be widely applicable to all families of porous ions and represents a new and powerful method for the synthesis of porous solids with tailored functionalities.

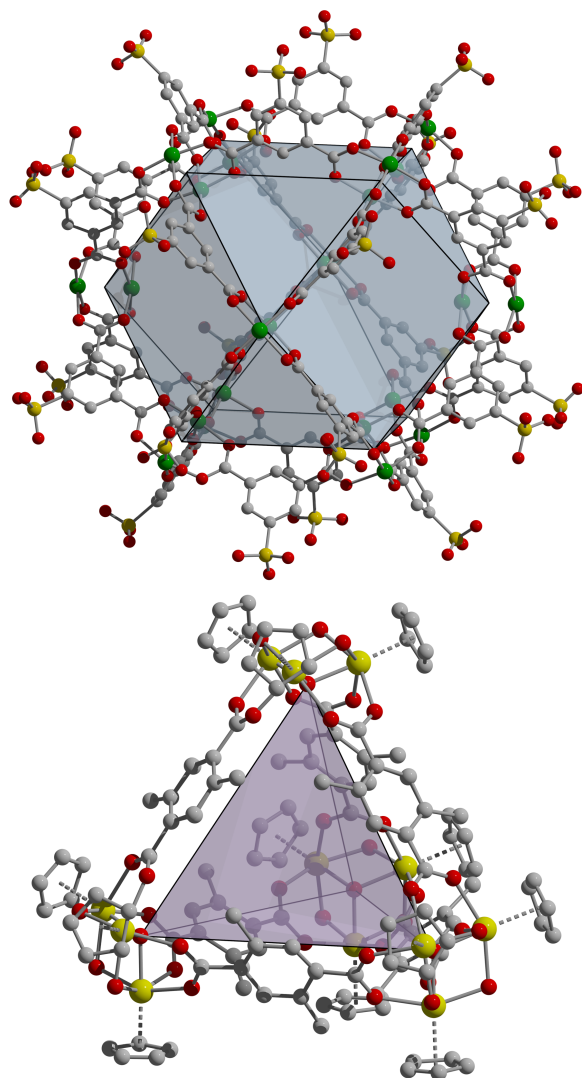
Over the past several decades, metal-organic frameworks (MOFs) have shown structural diversity that is unrivaled across competing classes of porous materials,<sup>1,2,3</sup> including zeolites,<sup>4,5</sup> activated carbons,<sup>6</sup> and all-organic adsorbents,<sup>7,8,9</sup> such as porous aromatic frameworks (PAFs) and covalent organic frameworks (COFs). This is largely a result of the rich coordination chemistry that can be used to precisely tune structural properties of MOFs. An endless number of organic bridging ligands can be combined with nearly every transition metal cation to afford solid adsorbents of limitless structure types.<sup>10,11</sup> This tunability has been leveraged to utilize MOFs for applications ranging from gas storage and separation to catalysis and sensing.<sup>12,13,14</sup> Further tunability in these materials has been recently achieved by targeting mixed ligand and/or mixed metal frameworks.<sup>15,16</sup> For both of these strategies, direct synthesis and post-synthetic modification have been employed.<sup>17,18</sup> For example, mixed-metal MOFs can be isolated by using mixed-functionality ligands where the different groups selectively coordinate specific metal cations.<sup>19</sup> Chelating groups can also be added and subsequently metallated post-synthetically.<sup>20,21</sup>

To date, however, many examples of mixed-functionality

frameworks have been fortuitous, where mixed-composition starting materials or reaction solutions may or may not afford mixed-composition products.<sup>22</sup> Porous cages may offer a benefit in this regard as their molecular nature allows for compatibility with mix and match strategies of higher fidelity.<sup>23,24,25,26</sup> Porous organic cages (POCs) have been previously used in this capacity in the isolation of so-called porous organic alloys. Here, POCs of different chirality are combined to make cocrystals with specificity at crystallographic sites based on the nature of the starting cage.<sup>27</sup> However, there are few examples of combining porous molecular species to reproducibly afford solid material of a controlled composition as solid solutions are often attained.<sup>28</sup> The work presented here describes a novel route to obtain mixed-functionality porous solids based on molecular starting materials. The functional groups, pore geometry, and metal cations in the product are tunable based on their presence in the starting charged cages. Further, the ratio of each component is potentially tunable based on the overall charge of the starting cages. A straightforward salt metathesis approach can be used to precipitate porous solids.

In choosing the starting cages for this approach, it was advantageous to target cages that fulfill both requirements of having the requisite charge and demonstrating the potential for permanent porosity. There are numerous examples of supramolecular complexes of varying charge that have been under investigation for decades.<sup>29–38</sup> A subset of these have recently been used in the development of porous ionic liquids.<sup>39</sup> Demonstration of permanent porosity in coordination cages is considerably less common.<sup>40,41</sup> This is particularly the case for charged coordination cages where porosity has been reported most consistently for the CIAC (Changchun Institute of Applied Chemistry),<sup>42,43</sup> MOSC (Metal-Organic Super Container),<sup>44,45</sup> and HMONC (Heterometallic Organic Nanocage)<sup>46</sup> families of cages in addition to the tetrahedral zirconium-based cages that have been recently under investigation by a number of groups.<sup>47,48,49,50</sup> Further, in order to be compatible with this salt metathesis approach, wherein solutions of oppositely charged cages are mixed to precipitate a porous salt, the starting cages must display high stability as well as solubility in various organic solvents. As the anionic component of the material, we chose the cuboctahedral, sulfonate-functionalized copper paddlewheel cage  $[\text{Cu}_{24}(\text{SO}_3\text{-bdc})_{24}]^{24-}$  as analogous cages that adopt

1 this structure type have shown some of the highest surface areas reported for coordination cages.<sup>51,52,53</sup> The highly-stable zirconium-based cage,  $[\text{Zr}_{12}(\mu_3\text{-O})_4(\mu_2\text{-OH})_{12}(\text{Cp})_{12}(\text{bdc})_6]\text{Cl}_4$ , was targeted as a result of its cationic charge, well established permanent porosity, and previously demonstrated amenability to post-synthetic modification strategies.<sup>54</sup>



21  
22  
23  
24  
25  
26  
27  
28  
29  
30  
31  
32  
33  
34  
35  
36  
37  
38  
39  
40  
41 **Figure 1.** Charged cages used for the preparation of a doubly-porous salt where the charge-balancing cations for the cuboctahedral cage  $[\text{Cu}_{24}(\text{SO}_3\text{-bdc})_{24}]^{24-}$  (upper) and anions for the tetrahedral cage  $[\text{Zr}_{12}(\mu_3\text{-O})_4(\mu_2\text{-OH})_{12}(\text{Cp})_{12}(\text{Me}_2\text{-bdc})_6]^{4+}$  (lower) are omitted for clarity. Green, light yellow, gray, red, and dark yellow atoms represent copper, zirconium, carbon, oxygen, and sulfur, respectively. Hydrogen atoms have been omitted. The colored polyhedra in the center of the cages represent potential pore volume on the interior surface of the cages.

42 Our efforts to scale the synthesis of  $[\text{Cu}_{24}(\text{SO}_3\text{-bdc})_{24}]^{24-}$ , which is most commonly isolated as a sodium salt, often resulted in the isolation of mixed phase or poorly-soluble products. We adopted a modified procedure for the synthesis of this cage where the mechanochemical reaction of copper(II) acetate monohydrate with the monolithium salt of 5-sulfoisophthalic acid afforded the target cage in nearly quan-

titative yield. Solvent exchange, activation, and recrystallization gave diffraction quality single crystals which confirmed the target cage was obtained (Figure 1). Similarly, although the reaction of  $\text{ZrCl}_2\text{Cp}_2$  and terephthalic acid in DMF afforded the tetrahedral structure,  $[\text{Zr}_{12}(\mu_3\text{-O})_4(\mu_2\text{-OH})_{12}(\text{Cp})_{12}(\text{bdc})_6]\text{Cl}_4$  in high yield, the moderate solubility of this cage necessitated anion exchange via reaction with silver triflate. Here, the reaction of  $[\text{Zr}_{12}(\mu_3\text{-O})_4(\mu_2\text{-OH})_{12}(\text{Cp})_{12}(\text{bdc})_6]\text{Cl}_4$  with  $\text{AgOTf}$  in methanol affords soluble  $[\text{Zr}_{12}(\mu_3\text{-O})_4(\mu_2\text{-OH})_{12}(\text{Cp})_{12}(\text{bdc})_6]\text{OTf}_4$  with concomitant precipitation of  $\text{AgCl}$ . However, NMR and mass spectrometry analysis of the product cage revealed a mixture of products with significant impurities of an unknown phase and lower than expected surface areas. We screened a variety of functionalized terephthalic acid ligands and ultimately discovered that utilization of the dimethyl-functionalized ligand, 2,5-dimethyl-bdc gives phase-pure cage  $[\text{Zr}_{12}(\mu_3\text{-O})_4(\mu_2\text{-OH})_{12}(\text{Cp})_{12}(\text{Me}_2\text{-bdc})_6]\text{Cl}_4$  (Figure 1). The presence of functional groups in the syntheses of the related UiO-66 framework has been shown to have a pronounced effect on the stability of the MOF.<sup>55</sup> The triflate salt of this cage,  $[\text{Zr}_{12}(\mu_3\text{-O})_4(\mu_2\text{-OH})_{12}(\text{Cp})_{12}(\text{Me}_2\text{-bdc})_6]\text{OTf}_4$  is similarly isolable via reaction with  $\text{AgOTf}$ .

43 With large quantities of oppositely-charge, potentially porous cages in hand, we pursued the synthesis of the doubly-porous salt. Both the starting cationic and anionic cages display appreciable solubility in a variety of solvents, including MeOH, formamide, and N,N-dimethylformamide. Combination of a dark blue solution of copper cage with a colorless solution of zirconium cage over the course of 30 minutes resulted in nearly instantaneous precipitation of a light-blue insoluble solid. Consistent with the rapid nature of precipitation, powder X-ray diffraction experiments indicated the product was amorphous. Scanning electron microscopy (Figure 2) corroborates this observation as the product has significantly smaller and less defined particles than the parent cages. Both X-ray photoelectron spectroscopy (XPS) and energy-dispersive X-ray (EDX) spectroscopy experiments confirm the presence of both zirconium and copper in the product phase (Figure 2). The precipitation of the product is expected to proceed with concomitant formation of lithium triflate, which is highly soluble in methanol. Accordingly, fluorine and lithium XPS and EDX confirm completion of the metathesis reaction as their absence verifies no triflate anion or lithium cation are present in the product salt. This suggests the resulting product material is nominally described is charged balanced based only on the presence of cage with a proposed formula of  $[\text{Zr}_{12}(\mu_3\text{-O})_4(\mu_2\text{-OH})_{12}(\text{Cp})_{12}(\text{Me}_2\text{-bdc})_6]_6[\text{Cu}_{24}(\text{SO}_3\text{-bdc})_{24}]$ .

44 Further spectroscopic characterization of these materials supports the proposed formulation (Figures S1-S9). Digestion and NMR analysis of the insoluble powder confirms the 24:36  $\text{Me}_2\text{-bdc}:\text{SO}_3\text{-bdc}$  ratio that is expected for a 6:1 zirconium:copper cage mixture. The infrared spectrum of the

product phase features prominent features of both pure starting cages. Here, strong IR bands at 1556, 1416, and 815  $\text{cm}^{-1}$  for the zirconium cage and 1196, 1118, and 1044  $\text{cm}^{-1}$  for the copper cage are evident in the product phase. Similarly, diffuse reflectance UV-vis spectra of the light-blue product phase displays absorbance maxima at 475 and 525 nanometers, which are present in the pure zirconium and copper cages, respectively. The salt phase is MOF-like in nature as it is completely insoluble in all organic solvents. Analogous to most MOFs, however, the salt decomposes in large quantities of water.

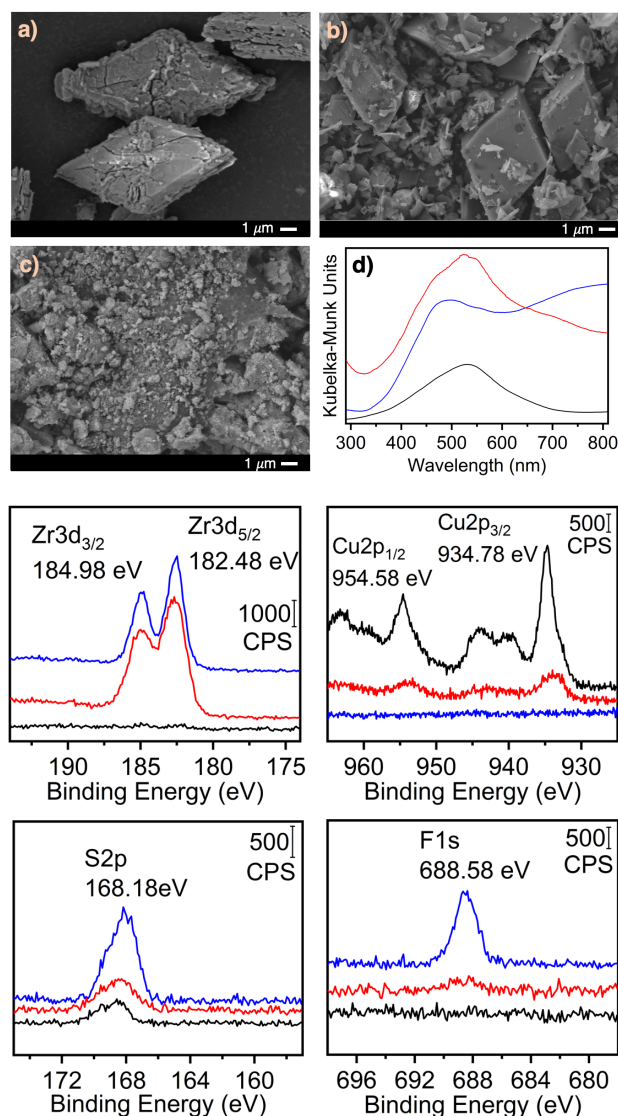


**Figure 2.** SEM images of  $\text{Li}_{24}[\text{Cu}_{24}(\text{SO}_3\text{-bdc})_{24}]$  (a),  $[\text{Zr}_{12}(\mu_3\text{-O})_4(\mu_2\text{-OH})_{12}(\text{Cp})_{12}(\text{Me}_2\text{-bdc})_6]\text{OTf}_4$  (b) and  $[\text{Zr}_{12}(\mu_3\text{-O})_4(\mu_2\text{-OH})_{12}(\text{Cp})_{12}(\text{Me}_2\text{-bdc})_6]_6[\text{Cu}_{24}(\text{SO}_3\text{-bdc})_{24}]$  produced from a 30 minute reaction (c). UV-vis spectra for starting cages and product (d). XPS spectra of the starting materials and product for the indicated element. For all spectra black = copper cage, blue = zirconium cage, and red = salt.

Isolation of a sample prepared in methanol, followed by further methanol washes to remove unreacted cage and lithi-

um triflate, followed by evacuation at 75  $^\circ\text{C}$  gives a material with an  $\text{N}_2$  accessible BET (Langmuir) surface area of 496 (1057)  $\text{m}^2/\text{g}$  (Figures S6-S8). Similarly,  $[\text{Zr}_{12}(\mu_3\text{-O})_4(\mu_2\text{-OH})_{12}(\text{Cp})_{12}(\text{Me}_2\text{-bdc})_6]_6[\text{Cu}_{24}(\text{SO}_3\text{-bdc})_{24}]$  has a  $\text{CO}_2$  accessible BET (Langmuir) surface area of 252 (593)  $\text{m}^2/\text{g}$ . The small particle sizes of the salt results in adsorption isotherms that reflect considerable external particle surface areas. Consistent with the removal of nonporous components from the starting materials, namely lithium cations and triflate anions, the product phase displays higher surface area than either of the starting cages.  $[\text{Zr}_{12}(\mu_3\text{-O})_4(\mu_2\text{-OH})_{12}(\text{Cp})_{12}(\text{Me}_2\text{-bdc})_6]\text{OTf}_4$  has a BET (Langmuir) surface area of 416 (606)  $\text{m}^2/\text{g}$  while  $\text{Li}_{24}[\text{Cu}_{24}(\text{SO}_3\text{-bdc})_{24}]$  is nonporous to  $\text{N}_2$ . For comparison, copper-based cuboctahedral cages have displayed BET surface areas ranging from nonporous to 739  $\text{m}^2/\text{g}$  while zirconium-based tetrahedral cages have shown BET surface areas from 104  $\text{m}^2/\text{g}$  to 782  $\text{m}^2/\text{g}$ .<sup>24,48,54,56,57,58</sup> We expect that judicious selection of charged starting cages will afford porous salts with even higher surface areas and tunable adsorption properties.

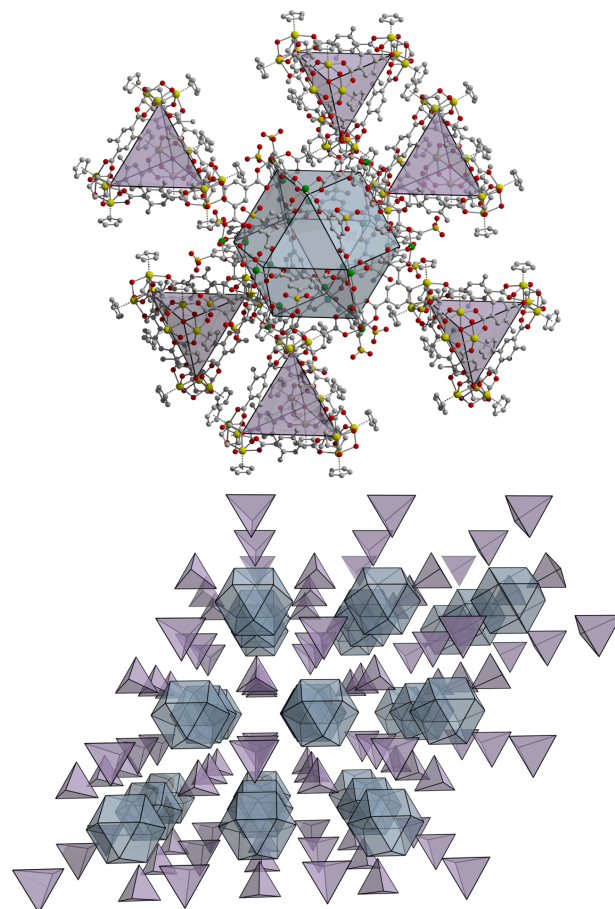


**Figure 3.** A portion of the crystal structure of the doubly porous salt  $\text{X}_{16}[\text{Zr}_{12}(\mu_3\text{-O})_4(\mu_2\text{-OH})_{12}(\text{Cp})_{12}(\text{Me}_2\text{-bdc})_6]_2[\text{Cu}_{24}(\text{SO}_3\text{-bdc})_{24}]$  where X is either  $\text{H}^+$  or  $\text{TEA}^+$ . Blue and purple polygons represent the copper cuboctahedral and zirconium tetrahedral cages, respectively. Hydrogen bonding between the sulfonate groups of the copper cage and bridging hydroxide groups of the zirconium cage result in crystallographic order.

In order to obtain single crystal diffraction quality crystals for structural analysis, a number of slow addition protocols were employed. Further, we surveyed tuning the starting cage counter ions and used the lithium, sodium, and tetraethylammonium salts of  $[\text{Cu}_{24}(\text{SO}_3\text{-bdc})_{24}]^{2+}$  in conjunction with the triflate, nitrate, and chloride salts of  $[\text{Zr}_{12}(\mu_3\text{-O})_4(\mu_2\text{-OH})_{12}(\text{Cp})_{12}(\text{Me}_2\text{-bdc})_6]^{4+}$ . Ultimately, layering of a methanol solution of  $\text{TEA}_{24}[\text{Cu}_{24}(\text{SO}_3\text{-bdc})_{24}]$  on a DMF solution of  $[\text{Zr}_{12}(\mu_3\text{-O})_4(\mu_2\text{-OH})_{12}(\text{Cp})_{12}(\text{Me}_2\text{-bdc})_6]\text{OTf}_4$  in an NMR tube for two weeks afforded diffraction quality single crystals of  $\text{X}_{16}[\text{Zr}_{12}(\mu_3\text{-O})_4(\mu_2\text{-OH})_{12}(\text{Cp})_{12}(\text{Me}_2\text{-bdc})_6]_2[\text{Cu}_{24}(\text{SO}_3\text{-bdc})_{24}]$  where X is either protons or tetraethylammonium cations. This structure, the first of its kind, is a salt where both the cations and anions are porous cages. Each cuboctahedral copper cage is surrounded by six tetrahedral zirconium cages. The tetrahedral cages are shared by neighboring copper cages via hydrogen bonding between the bridging hydroxide groups on the tetrahedra and the sulfonate groups, giving a total Zr:Cu cage ratio of 2:1. It is notable that the Zr:Cu cage ratio for a product formed over the course of two weeks is significantly smaller than that obtained via mixing for 30 minutes. In preparing amorphous powders, samples with lower than the 6:1 ratio were isolated when  $\text{Li}^+$  salts of the starting copper cage were allowed to react for longer than 30 minutes. As determined by NMR digestion and EDX spectroscopy, reaction mixtures stirred for 150 and 300 minutes gave powders with Cu:Zr cage ratios of 5:1 and 4.7:1, respectively. Interestingly, and consistent with the single-crystal diffraction experiments, utilization of a twofold excess of Zr cages also gave product with similar Zr:Cu cage ratio (4.9:1) as confirmed by EDX and NMR analysis. As expected, utilization of a twofold excess of copper cage afforded a sample with a further reduced Zr cage content (3:1 ratio).

In conclusion, we have shown that the combination of potentially porous ionic cages can be used to prepare porous salts where both the cation and anion are based on porous cages. For the particular adsorbents reported here, the ratio of cationic cage to anionic cage is tunable based on the length of mixing time of products with the longest reaction affording insoluble  $\text{X}_{16}[\text{Zr}_{12}(\mu_3\text{-O})_4(\mu_2\text{-OH})_{12}(\text{Cp})_{12}(\text{Me}_2\text{-bdc})_6]_2[\text{Cu}_{24}(\text{SO}_3\text{-bdc})_{24}]$  and the fastest addition giving the pure-cage salt  $[\text{Zr}_{12}(\mu_3\text{-O})_4(\mu_2\text{-OH})_{12}(\text{Cp})_{12}(\text{Me}_2\text{-bdc})_6]_6[\text{Cu}_{24}(\text{SO}_3\text{-bdc})_{24}]$ . The porous salts display moderate surface area which is higher than those of its constituent cages. It is our expectation that the design and synthesis strategies outlined here will be useful for the isolation of an even further expanded class of porous cage materials utilizing the large library of porous, or potentially-porous, charged coordination cages.

## ASSOCIATED CONTENT

The Supporting Information is available free of charge on the ACS Publications website.

Detailed experimental procedures, gas adsorption data, X-ray diffraction data, structure figures, mass spectrometry data, and spectroscopic data. (PDF)

## AUTHOR INFORMATION

### Corresponding Author

\*E-mail: edb@udel.edu.

### Notes

No competing financial interests have been declared.

## ACKNOWLEDGMENT

This material is based upon work supported by the U.S. Department of Energy's Office of Energy Efficiency and Renewable Energy under the Hydrogen and Fuel Cell Technologies and Vehicle Technologies Offices under Award Number DE-EE0008813. We thank the DOE Office of Science Graduate Student Research (SCGSR) Program for fellowship support of E.J.G. We also thank Jian Zhang for assistance with single-crystal X-ray diffraction experiments.

## REFERENCES

- (1) Xuan, W.; Zhu, C.; Liu, Y.; Cui, Y. Mesoporous metal-organic framework materials. *Chem. Soc. Rev.* **2012**, *41*, 1677-1695.
- (2) Furukawa, H.; Cordova, K. E.; O'Keeffe, M.; Yaghi, O. M. The Chemistry and Applications of Metal-Organic Frameworks. *Science*. **2013**, *341*, 974-988.
- (3) Gangu, K. K.; Maddila, S.; Mukkamala, S. B.; Jonnalagadda, S. B. A review on contemporary Metal-Organic Framework materials. *Inorganica. Chim. Acta*. **2016**, *446*, 61-74.
- (4) Li, J.; Corma, A.; Yu, J. Synthesis of new zeolite structures. *Chem. Soc. Rev.* **2015**, *44*, 7112-7127.
- (5) Rangekar, N.; Mittal, N.; Elyassi, B.; Caro, J.; Tsapatsis. Zeolite membranes - a review and comparison with MOFs. *Chem. Soc. Rev.* **2015**, *44*, 7128-7154.
- (6) Shafeeyan, M. S.; Duad, W. M. A. W.; Houshmand, A.; Shamiri, A. A review on surface modification of activated carbon for carbon dioxide adsorption. *J. Anal. Appl. Pyrol.* **2010**, *89*, 143-151.
- (7) Diaz, U.; Corma, A. Ordered covalent organic frameworks, COFs and PAFs. From preparation to application. *Coord. Chem. Rev.* **2016**, *311*, 85-124.
- (8) Zeng, Y.; Zou, R.; Zhao, Y. Covalent Organic Frameworks for  $\text{CO}_2$  Capture. *Adv. Mater.* **2016**, *28*, 2855-2873.
- (9) Huang, J.; Turner, S. R.; Hypercrosslinked Polymers: A Review. *Polym. Rev.* **2017**, *58*, 1-41.
- (10) Stock, N.; Biswas, S. Synthesis of Metal-organic Frameworks (MOFs): Routes to Various MOF Topologies, Morphologies, and Composites. *Chem. Rev.* **2012**, *112*, 933-969.
- (11) Lee, Y.-R.; Ahn, W.-S. Synthesis of metal-organic frameworks: A mini review. *Korean J. Chem. Eng.* **2013**, *30*, 1667-1680.
- (12) Li, H.; Wang, K.; Sun, Y.; Lollar, C. T.; Li, J. Zhou, H.-C. Recent advances in gas storage and separation using metal-organic frameworks. *Mater. Today*. **2018**, *21*, 108-121.
- (13) Huang, Y.-B.; Lian, J.; Wang, X.-S.; Cao, R. Multifunctional metal-organic framework catalysts: synergistic catalysis and tandem reactions. *Chem. Soc. Rev.* **2017**, *46*, 126-157.
- (14) Kumar, P.; Deep, A.; Kim, K.-H. Metal organic frameworks for sensing applications. *Trac-trend. Anal. Chem.* **2015**, *73*, 39-53.
- (15) Dhakshinamoorthy, A.; Asiri, A. M.; Garcia, H. Mixed-metal or mixed-linker metal organic frameworks as heterogeneous catalysts. *Catal. Sci. Technol.* **2016**, *6*, 5238-5261.
- (16) Du, M.; Li, C.-P.; Liu, C.-S.; Fang, S.-M. Design and construction of coordination polymers with mixed-ligand synthetic strategy. *Coord. Chem. Rev.* **2013**, *257*, 1282-1305.

- (17) Cao, T.; Peng, Y.; Liu, T.; Wang, S.; Dou, J.; Li, Y.; Zhou, C.; Li, D.; Bai, J. Assembly of a series of d10 coordination polymers of pamoic acid through a mixed-ligand synthetic strategy: synthesis, structures and fluorescence properties. *CrystEngComm*. **2014**, *46*, 10658-10673.
- (18) Wang, Z.; Tanabe, K. K.; Cohen, S. M. Accessing Postsynthetic Modification in a Series of Metal-Organic Frameworks and the Influence of Framework Topology on Reactivity. *Inorg. Chem.* **2009**, *48*, 296-306.
- (19) Yang, X.-L.; Zou, C.; He, Y.; Zhao, M.; Chen, B.; Xiang, S.; O'Keeffe, M.; Wu, C.-D. A Stable Microporous Mixed-Metal Metal-organic Framework with Highly Active Cu<sup>2+</sup> Sites for Efficient Cross-Dehydrogenative Coupling Reactions. *Chem. Eur. J.* **2014**, *20*, 1447-1452.
- (20) Ma, L.; Falkowski, J. M.; Abney, C.; Lin, W. A series of isorecticular chiral metal-organic frameworks as a tunable platform for asymmetric catalysis. *Nat. Chem.* **2010**, *2*, 838-846.
- (21) Das, M. C.; Xiang, S.; Zhang, Z.; Chen, B. Functional Mixed Metal-Organic Frameworks with Metalloligands. *Angew. Chem. Int. Ed.* **2011**, *50*, 10510-10520.
- (22) Abednatanzi, S.; Derakhshandeh, P. G.; Depauw, H.; Coudert, F.-X.; Vrielinck, H.; Voort, P. V. D.; Leus, K. Mixed-metal metal-organic frameworks. *Chem. Soc. Rev.* **2019**, *48*, 2535-2565.
- (23) Hasell, T.; Chong, S. Y.; Jelfs, K. E.; Adams, J. D.; Cooper, A. I. Porous Organic Cage Nanocrystals by Solution Mixing. *J. Am. Chem. Soc.* **2012**, *134*, 588-598.
- (24) Nam, D.; Huh, J.; Lee, J.; Kwak, J. H.; Jeong, H. Y.; Choi, K.; Choe, W. Cross-linking Zr-based metal-organic polyhedra via postsynthetic polymerization. *Chem. Sci.* **2017**, *8*, 7765-7771.
- (25) Fulong, C. R. P.; Liu, J.; Pastore, V. J.; Lin, H.; Cook, T. R. Mixed-matrix materials using metal-organic polyhedra with enhanced compatibility for membrane gas separation. *Dalton Trans.* **2018**, *47*, 7905-7915.
- (26) Carne-Sanchez, A.; Albalad, J.; Grancha, T.; Imaz, I.; Juanhuix, J.; Larpent, P.; Furukawa, S.; Maspocho, D. Postsynthetic Covalent and Coordination Functionalization of Rhodium(II)-Based Metal-Organic Polyhedra. *J. Am. Chem. Soc.* **2019**, *141*, 4094-4102.
- (27) Hasell, T.; Cooper, A. I.; Porous organic cages: soluble, modular and molecular pores. *Nat. Rev. Mater.* **2016**, *1*, 16053.
- (28) Hasell, T.; Chong, S. Y.; Schmidtman, M.; Adams, D. J.; Cooper, A. I. Porous organic alloys. *Angew. Chem. Int. Ed.* **2012**, *51*, 7154-7157.
- (29) Percastegui, E. G.; Mosquera, J.; Ronson, T. K.; Plajer, A. J.; Kieffer, M.; Nitschke, J. R. Waterproof architectures through subcomponent self-assembly. *Chem. Sci.* **2019**, *10*, 2006-2018.
- (30) Cook, T. R.; Stang, P. J. Recent Developments in the Preparation and Chemistry of Metallacycles and Metallacages via Coordination. *Chem. Rev.* **2015**, *115*, 7001-7045.
- (31) Frank, M.; Johnstone, M. D.; Clever, G. H. Interpenetrated Cage Structures. *Chem. Eur. J.* **2016**, *22*, 14104-14125.
- (32) Hiraoko, S.; Fujita, M. Guest-Selected Formation of Pd(II)-Linked Cages from a Prototypical Dynamic Library. *J. Am. Chem. Soc.* **1999**, *121*, 10239-10240.
- (33) Seidel, S. R.; Stang, P. J. High-Symmetry Coordination Cages via Self-Assembly. *Acc. Chem. Res.* **2002**, *35*, 972-983.
- (34) Yeh, R. M.; Xu, J.; Seeber, G.; Raymond, K. N. Large M<sub>4</sub>L<sub>4</sub> (M = Al(III), Ga(III), In(III), Ti(IV)) Tetrahedral Coordination Cages: an Extension of Symmetry-Based Design. *Inorg. Chem.* **2005**, *44*, 6228-6239.
- (35) Wang, Z. J.; Brown, C. J.; Bergman, R. G.; Raymond, K. N.; Toste, F. D. Hydroalkoxylation Catalyzed by a Gold(I) Complex Encapsulated in a Supramolecular Host. *J. Am. Chem. Soc.* **2011**, *133*, 7358-7360.
- (36) Oldacre, A. N.; Friedman, A. E.; Cook, T. R. A Self-Assembled Co-facial Cobalt Porphyrin Prism for Oxygen Reduction Catalysis. *J. Am. Chem. Soc.* **2017**, *139*, 1424-1427.
- (37) Grommet, A. B.; Bolliger, J. L.; Brown, C.; Nitschke, J. R. A Triphasic Sorting System: Coordination Cages in Ionic Liquids. *Angew. Chem. Int. Ed.* **2015**, *54*, 15100-15104.
- (38) Black, S. P.; Wood, D. M.; Schwarz, F. B.; Ronson, T. K.; Holstein, J. J.; Stefankiewicz, A. R.; Schalley, C. A.; Sanders, J. K. M.; Nitschke, J. R. Catenation and encapsulation induce distinct reconstitutions within a dynamic library of mixed-ligand Zn<sub>4</sub>L<sub>6</sub> cages. *Chem. Sci.* **2016**, *7*, 2614-2620.
- (39) Ma, L.; Haynes, C. J. E.; Grommet, A. B.; Walczak, A.; Parkins, C. C.; Doherty, C. M.; Longley, L.; Tron, A.; Stefankiewicz, A. R.; Bennett, T. D.; Nitschke, J. R. Coordination cages as permanently porous ionic liquids. *Nat. Chem.* **2020**, *12*, 270-275.
- (40) Dalgarno, S. J.; Power, N. P.; Atwood, J. L. Metallo-supramolecular capsules. *Coord. Chem. Rev.* **2008**, *252*, 825-841.
- (41) Vardhan, H.; Yusubov, M.; Verpoort, F. Self-assembled metal-organic polyhedra: An overview of various applications. *Coord. Chem. Rev.* **2016**, *306*, 171-194.
- (42) Liu, M.; Liao, W. Bridging calixarene-based {Co<sub>4</sub>} units into a square or belt with aromatic dicarboxylic acids. *CrystEngComm*. **2012**, *14*, 5727-5729.
- (43) Du, S.; Hu, C.; Xiao, J.-C.; Tan, H.; Liao, W. A giant coordination cage based on sulfonylcalix[4]arenes. *Chem. Commun.* **2012**, *48*, 9177-9179.
- (44) Dai, F.-R.; Sambasivam, U.; Hammerstrom, A. J.; Wang, Z. Synthetic Supercontainers Exhibit Distinct Solution versus Solid State Guest-Binding Behavior. *J. Am. Chem. Soc.* **2014**, *136*, 7480-7491.
- (45) Dai, F.-R.; Wang, Z. Modular Assembly of Metal-Organic Supercontainers Incorporating Sulfonylcalixarenes. *J. Am. Chem. Soc.* **2012**, *134*, 8002-8005.
- (46) Su, K.; Jiang, F.; Qian, J.; Chen, L.; Pang, J.; Bawaked, S. M.; Mokhtar, M.; Al-Thabaiti, S. A.; Hong, M. Stepwise Construction of Extra-Large Heterometallic Calixarene-Based Cages. *Inorg. Chem.* **2015**, *54*, 3183-3188.
- (47) Liu, G.; Yuan, Y. D.; Wang, J.; Cheng, Y.; Peh, S. B.; Wang, Y.; Qian, Y.; Dong, J.; Yuan, D.; Zhao, D. Process-Tracing Study on the Postassembly Modification of Highly Stable Zirconium Metal-Organic Cages. *J. Am. Chem. Soc.* **2018**, *140*, 6231-6234.
- (48) Jiao, J.; Tan, C.; Li, Z.; Liu, Y.; Han, X.; Cui, Y. Design and Assembly of Chiral Coordination Cages for Asymmetric Sequential Reactions. *J. Am. Chem. Soc.* **2018**, *140*, 2251-2259.
- (49) Liu, G.; Zeller, M.; Su, K.; Pang, J.; Ju, Z.; Yuan, D.; Hong, M. Controlled Orthogonal Self-Assembly of Heterometal-Decorated Coordination Cages. *Chem. Eur. J.* **2016**, *22*, 17345-17350.
- (50) Xing, W.-H.; Li, H.-Y.; Dong, X.-Y.; Zang, S.-Q. Robust multifunctional Zr-based metal-organic polyhedra for high proton conductivity and selective CO<sub>2</sub> capture. *J. Mater. Chem. A.* **2018**, *6*, 7724-7730.
- (51) Lorzing, G. R.; Gosselin, E. J.; Trump, B. A.; York, A. H. P.; Sturluson, A.; Rowland, C. A.; Yap, G. P. A.; Brown, C. M.; Simon, C. M.; Bloch, E. D. Understanding Gas Storage in Cuboctahedral Porous Coordination Cages. *J. Am. Chem. Soc.* **2019**, *141*, 12128-12138.
- (52) Lorzing, G. R.; Trump, B. A.; Brown, C. M.; Bloch, E. D. Selective Gas Adsorption in Highly Porous Chromium (II)-Based Metal-Organic Polyhedra. *Chem. Mater.* **2017**, *29*, 8583-8587.
- (53) Park, J.; Perry, Z.; Chen, Y.-P.; Bae, J.; Zhou, H.-C. Chromium(II) Metal-Organic Polyhedra as highly Porous Materials. *ACS Appl. Mater. Interfaces.* **2017**, *9*, 28064-28068.
- (54) Liu, G.; Ju, Z.; Yuan, D.; Hong, M. In Situ Construction of a Coordination Zirconocene Tetrahedra. *Inorg. Chem.* **2012**, *52*, 13815-13817.
- (55) Huang, Y.; Qin, W.; Li, Z.; Li, Y. Enhanced stability and CO<sub>2</sub> affinity of a UiO-66 type metal-organic framework decorated with dimethyl groups. *Dalton Trans.* **2012**, *41*, 9283-9285.
- (56) Liu, T. -F. F.; Chen, Y.-P. P.; Yakovenko, A. A.; Zhou, H.-C. Interconversion between Discrete and a Chain of Nanocages: Self-Assembly via a Solvent-Driven, Dimension-Augmentation Strategy. *J. Am. Chem. Soc.* **2012**, *134*, 17358-17361.
- (57) Barreda, O.; Bannwart, G.; Yap, G. P. A.; Bloch, E. D. Ligand-Based Phase Control in Porous Molecular Assemblies. *ACS Appl. Mater. Interfaces* **2018**, *10*, 11420-11424.
- (58) Sun, L. -B.; Li, J. -R.; Lu, W.; Gu, Z. -Y.; Luo, Z.; Zhou, H. -C. Confinement of Metal-Organic Polyhedra in Silica Nanopores. *J. Am. Chem. Soc.* **2012**, *134*, 15923-15928.

